

To appear in *Astrophysical Journal*: accepted February 7,
2002

Star Clusters as Type Ia Supernova Factories

Michael M. Shara and Jarrod R. Hurley

*Department of Astrophysics, American Museum of Natural History, Central Park West at
79th Street,
New York, NY 10024*

mshara@amnh.org, jhurley@amnh.org

ABSTRACT

We find a remarkably enhanced production rate in star clusters (relative to the field) of very short period, massive double-white-dwarf stars and of giant-white dwarf binaries. These results are based on N -body simulations performed with the new GRAPE-6 special purpose hardware and are important in identifying and characterizing the progenitors of type Ia supernovae. The high incidence of very close double-white-dwarf systems is the result of dynamical encounters between (mostly) primordial binaries and other cluster stars. Orbital hardening rapidly drives these degenerate binaries to periods under ~ 10 hours. Gravitational radiation emission and mergers producing supra-Chandrasekhar objects follow in less than a Hubble time. If most stars are born in clusters then estimates of the double white dwarf merger rates in galaxies (due to cluster dynamical interaction) must be increased more than tenfold. A majority of the Roche lobe overflow giant-white dwarf binaries are not primordial; they are produced in exchange reactions. Most cases resulted in a common-envelope and formation of a double-white-dwarf binary rather than Supersoft X-ray sources leading possibly to a type Ia supernova.

Subject headings: stellar dynamics—methods: N -body simulations— type Ia supernovae—globular clusters: general— open clusters and associations: general

1. Introduction

Type Ia supernovae (SNeIa) have recently been used to demonstrate that the Universe is apparently not only expanding, but also accelerating (Riess et al. 1998; Perlmutter et

al. 1999). If this remarkable discovery survives careful scrutiny it has profound implications for cosmology physics (see Leibundgut 2001 for a review). However, before accepting such a revolutionary change in our view of the universe, it is critical to investigate all challenges to the acceleration interpretation of the data. A thorough compilation of those challenges is given by Riess (2000).

Riess (2000) cites evolution, dust, gravitational lensing, measurement biases, selection biases and alternative cosmological models as potential challenges to the acceleration interpretation of the Type Ia supernova (SNIa) observations. He concludes that the primary source of reasonable doubt is evolution (could SNeIa at redshift $z = 0.5$ be intrinsically fainter than nearby SNeIa by 25%?). We simply don't know for certain what kind of star (or stars?) give rise to these explosions, and hence whether to expect systematic variations in SNIa luminosities with z .

Not knowing the progenitors of SNeIa is embarrassing because of the significant empirical corrections one must apply to supernova luminosities, based on their light curves, to get distances (Phillips 1993). If one could determine the SNIa progenitor with a high degree of reliability, one could build increasingly sophisticated supernova light curve models. This would lead to a fundamental understanding of the physical behavior of one of the most crucial standard candles in cosmology.

Two competing SNIa models exist: merging double-white-dwarfs (DWDs) and accreting single white dwarfs (ASDs) in close binary systems (see Yungelson & Livio 2000 for a review, including the pros and cons of each flavor of each model). In both cases the model involves the thermonuclear disruption of a white dwarf, most likely of carbon-oxygen (CO) composition, when its mass reaches, or exceeds, the critical Chandrasekhar mass. However, Saio & Nomoto (1998) have raised the possibility that supra-Chandrasekhar mass-accreting white dwarfs will undergo accretion-induced collapse (AIC) and the formation of a neutron star, rather than a SNIa. An important example of why it is so critical to know the progenitors of SNeIa is the following. ASDs accreting helium result in the accumulation of a He layer and an edge lit detonation; the peak luminosity-light curve shape relation of such objects may vary significantly with metallicity and hence redshift (Tout et al. 2001).

It is clearly important to calculate the expected incidence of DWDs and ASDs in the stellar populations of the different types of galaxies where SNIa occur. This has been done for field stars (Yungelson et al. 1996, for example), but hardly for the environs of clusters. We have begun this study, and find that dynamics dramatically alter binary populations and characteristics, including those of DWDs and ASDs. Such an effect has been predicted in the past (Chen & Leonard 1993) but has yet to be tested by direct means.

Many, and possibly all, stars were born in a star cluster (Kraft 1983; Lada, Strom & Myers 1993), or at the very least a loose association (Makarov & Fabricius 2001, for example). Living in an environment with stellar densities of $10^2 \text{ stars pc}^{-3}$ to as high as $10^7 \text{ stars pc}^{-3}$ can dramatically affect the evolution of stars. Physical collisions, and, in the case of binaries, exchange interactions or disruptions of orbits can radically alter the fates of cluster stars. The most direct way to model the evolution of a star cluster is with an N -body code in which the individual orbits of each star are followed in detail *and* the internal evolution of each star is also taken into account (Hurley et al. 2001).

We have begun a study of the behavior of populous star clusters using a state-of-the-art N -body code in conjunction with the powerful GRAPE-6 special purpose computer (Makino 2001). This will ultimately involve a large number of N -body simulations covering a wide range of initial conditions, e.g. metallicity, binary fraction, and stellar number density. A related study investigating the fate of planetary systems in star clusters is also ongoing (Hurley & Shara 2002). The remarkable evolution of close binaries comprised of one or two degenerate members is the focus of this early work. The increased importance of SNIa for cosmology makes these initial results particularly relevant to the scientific community.

Our simulation method is presented in Section 2, and the double white dwarfs are described in Section 3. The accreting white dwarfs are detailed in Section 4. We briefly summarize our results in Section 5.

2. Simulation Method

We have carried out simulations with 22 000 stars and a 10% primordial binary fraction using the Aarseth **NBODY4** code (Aarseth 1999; Hurley et al. 2001). A GRAPE-6 board located at the American Museum of Natural History hosts the code. This special purpose computer acts as a Newtonian force accelerator for N -body calculations, performing at 0.5 Tflops for a 16-chip board (~ 30 Gflops per chip).

The prescription used for single star evolution in **NBODY4** is described in Hurley, Pols & Tout (2000). A feature of this algorithm is the inclusion of metallicity as a free parameter, making it applicable to modelling clusters of all ages. It covers all stages of the evolution from the zero-age main-sequence (ZAMS) up to, and including, remnant stages such as the white dwarf cooling track. In terms of examining DWDs as SNIa candidates it is important to note that the WD initial-final mass relation found by Hurley, Pols & Tout (2000, see their Fig. 18) is well matched to observations.

All aspects of standard binary evolution, i.e. non-perturbed orbits, are treated ac-

cording to the prescription described in Hurley, Tout & Pols (2002). This includes tidal circularization and synchronization of the orbit, mass transfer, and angular momentum loss mechanisms such as magnetic braking and gravitational radiation. The default input parameters to this algorithm (listed in Table 3 of Hurley, Tout & Pols 2002) are adopted. In particular, this means that the common-envelope (CE) efficiency parameter is taken to be $\alpha_{\text{CE}} = 3.0$ which makes the outcome of common-envelope evolution similar to the alternative, and commonly used, scenario described by Iben & Livio (1993) with $\alpha_{\text{CE}} = 1.0$. Common-envelope evolution occurs when mass transfer develops on a dynamical timescale. In the evolution algorithm this equates to the donor star, generally a giant, having an appreciable convective envelope and a mass-ratio, q , exceeding some critical value, $q_{\text{crit}} \simeq 0.7$. If the conditions for dynamical mass-transfer are met then the envelope of the giant overfills the Roche-lobes of both stars leaving the giant core and the secondary star contained within a common-envelope. Owing to orbital friction these will spiral together and transfer energy to the envelope with an efficiency α_{CE} . If this process releases sufficient energy to drive off the entire envelope the outcome will be a close binary consisting of the giant core and the secondary, otherwise it leads to coalescence of the two objects.

Various models for binary evolution exist (Portegies Zwart & Verbunt 1996; Tutukov & Yungelson 1996; Tout et al. 1997, for example) with each having the similar goal of providing a sufficiently detailed description of binary behaviour while remaining computationally efficient. The main difference between these and the Hurley, Tout & Pols (2002) model referred to in this work, and incorporated in to NBODY4, is the much improved treatment of tidal interactions present in the latter. Tidal friction arising from convective, radiative or degenerate damping mechanisms is modelled and necessarily the stellar spins, which are subject to tidal circularization and synchronization, are followed for each star. Also, by using the single star evolution algorithm of Hurley, Pols & Tout (2000) the Hurley, Tout & Pols (2002) binary prescription not only allows for a wider range of evolution phases, with many of these modelled in more detail and based on updated stellar models, but can also be used to evolve binaries of any metallicity. An additional difference is that models such as those of Portegies Zwart & Verbunt (1996) and Tutukov & Yungelson (1996) follow the Iben & Livio (1993) common-envelope scenario while Hurley, Tout & Pols (2002) utilise the scenario first described in Tout et al. (1997). Subtle variations also exist from model to model in the way that various aspects of mass transfer are dealt with.

Gravitational radiation is an important process in the evolution of close binary systems because it provides a mechanism for removing angular momentum and driving the system towards a mass transfer state, possibly followed by coalescence. In the Hurley, Tout & Pols (2002) binary model orbital changes due to gravitational radiation are calculated using expressions based on the weak-field approximation of general relativity (Eggleton 2002) and

assuming the stars are point masses. This includes a strong dependence on the eccentricity of the orbit, although DWD systems are generally circular.

In the dense environment of a star cluster it is possible for the orbital parameters of a binary to be significantly perturbed owing to close encounters with nearby stars. It is even possible for the orbit to become chaotic as a result of such an interaction. Modelling of such events has been considered in detail by Mardling & Aarseth (2001) whose work is included in NBODY4. Three-body and higher-order subsystems are also followed in detail (Aarseth 1999, and references within).

We include the outcome of four simulations in the results described below and in Tables 1-3. The first two simulations were carried out assuming a metallicity of $Z = 0.004$, while the third and fourth simulations had $Z = 0.02$. In all other respects the initial conditions were identical for each simulation. Masses for single stars are chosen from the initial mass function (IMF) of Kroupa, Tout & Gilmore (1993) within the limits of $0.1 - 50M_{\odot}$. For primordial binaries the total mass of the binary is chosen from the IMF of Kroupa, Tout & Gilmore (1991), as this was not corrected for the effect of binaries, between the limits of $0.2 - 100M_{\odot}$. The component masses are then assigned according to a uniform distribution of mass-ratio, taking care to ensure that the single star mass limits are not violated. Following Eggleton, Fitchett & Tout (1989) we take the distribution of orbital separations for the primordial binaries to be

$$\left(\frac{a}{a_m}\right)^{\beta} = \sec(kW) + \tan(kW) , \quad (1)$$

where $W \in [-1, 1]$, and uniformly distributed and k satisfies

$$\sec k = \frac{1}{2} [\zeta^{\beta} + \zeta^{-\beta}] . \quad (2)$$

This distribution is symmetric in $\log a$ about a peak at a_m and ranges from a minimum separation of ζa_m to a maximum of a_m/ζ . We choose the constants ζ and β to be 10^{-3} and 0.33 respectively, and take $a_m \simeq 30$ AU, i.e. each separation, a , is within the range $\sim 6 R_{\odot}$ to 30 000 AU. The eccentricity of each binary orbit is taken from a thermal distribution (Heggie 1975). Initial positions and velocities of the stars are assigned according to a Plummer model (Aarseth, Hénon & Wielen 1974) in virial equilibrium.

Each simulation started with 18 000 single stars and 2 000 binaries and was evolved to an age of 4.5 Gyr when $\sim 25\%$ of the initial cluster mass remained and the binary fraction was still close to 10%. In real time each individual simulation took approximately five days to complete, which corresponds to $\sim 10^3$ cluster crossing-times, and $\sim 10^{17}$ floating-point operations on the GRAPE board. Clusters are evolved subject to a standard three-dimensional Galactic tidal field (see Hurley et al. 2001) of standard, i.e. local, strength

(Chernoff & Weinberg 1990, for example) so, in addition to mass loss from stellar evolution, mass is removed from the cluster when stars cross the tidal boundary and are lost to the Galaxy. Because the orbits of some bound stars may momentarily take them outside of the cluster, stars are not actually removed from the simulation until their distance from the cluster centre exceeds twice the tidal radius. At any moment in time less than 2% of the mass in a simulation is found to lie outside of the tidal radius and this has little effect on the evolution of the model (Giersz & Heggie 1997). Typically the velocity dispersion of the stars in these model clusters was 2 km s^{-1} with a core density of $10^3 \text{ stars pc}^{-3}$. The density of stars at the half-mass radius is generally a factor of 10 less than this. These simulations are clearly in the open cluster regime.

3. Double White Dwarfs

Double white dwarf systems must form in all stellar populations with binaries. To form short-period systems isolated binaries must undergo considerable common envelope evolution to shed angular momentum and bring their degenerate components close together. Only when the orbital period of a DWD is less than about 10 hours will gravitational radiation force the system to merge in less than the age of the universe. *A key result of this paper is that DWDs formed in clusters can be significantly hardened by interactions with passing stars. Alternatively, hardening of binaries before they reach the DWD stage, and/or exchange interactions, can produce a short-period DWD that would not have formed in isolation. This greatly increases the number of DWDs which merge in less than a Hubble time.* Heggie (1975) defined hard binaries to be sufficiently close that their binding energy exceeds the mean kinetic energy of the cluster stars. A binary is said to *harden* when an interaction with a third body removes energy from the orbit and thus reduces the separation. Three-body interactions may also lead to an exchange in which one of the binary components is displaced by the incoming third star. If an exchange does occur then the expelled star, generally the least massive, invariably leaves the three-body system altogether. Note that four-body interactions involving a second binary are also possible. The likelihood of a binary being the target of an exchange interaction scales linearly with the orbital separation of the binary (Heggie, Hut & McMillan 1996) and is also more likely to occur in the core of a cluster. Table 1 lists the characteristics of the merging DWDs formed during the four cluster simulations: epoch of formation, types of white dwarf, component and system masses, orbital period at formation epoch, gravitational inspiral timescale, and whether the binary is primordial or due to an exchange. All of these objects will merge in less than a Hubble time, creating a supra-Chandrasekhar object which may yield a SNIa.

From binary population synthesis alone we expect about 10 DWDs to be present amongst 2000 binaries of solar metallicity after 4 Gyr of evolution. This expected number rises to 15 DWDs for $Z = 0.004$ which is mainly a reflection of the accelerated evolution timescale for low metallicity stars with masses less than $\sim 9M_{\odot}$: the main-sequence (MS) lifetime for stars of Population II composition is roughly a factor of two shorter than for stars of solar composition (see Fig. 4 of Hurley, Pols & Tout 2000). Of these DWDs, only $\sim 0.2 - 0.3$ are expected to be a “loaded gun”, i.e. to have a combined mass, M_b , greater than the Chandrasekhar mass, $M_{\text{Ch}} \simeq 1.44$, and a merger timescale less than the age of the Galaxy (Hurley, Tout & Pols 2002). These population synthesis results refer to *isolated* binaries with initial conditions drawn from the same distributions as used in the N -body simulations presented here. From Table 1 we see that there are, on average, four “loaded guns” per 2000 binaries, which is ~ 15 times more than expected in a binary population unaffected by dynamical interactions. We note CO-CO DWDs dominate, but that CO-ONe binaries are also common (5 of 16 binaries). The system total masses range from $1.49M_{\odot}$ to $1.96M_{\odot}$. This range in masses and compositions suggests diversity in the light curves and spectra of the merging objects, whether or not they make SNIa.

Figure 1 highlights the evolution of two of the SNIa candidates formed in the simulations. The binary shown in the top panel of the figure is the DWD formed at 334 Myr in the first $Z = 0.004$ simulation (fourth entry in Table 1). This began as a primordial binary with component masses of $5.82M_{\odot}$ and $3.13M_{\odot}$, an eccentricity of 0.74, and an orbital period of 2138 d. It underwent two common-envelope events, the first at 76 Myr when the $5.82M_{\odot}$ star filled its Roche-lobe on the asymptotic giant branch (by which time tides raised on the convective envelope of the primary had circularized the orbit) and became an ONe WD, and the second at 232 Myr when the $3.13M_{\odot}$ star filled its Roche-lobe on the first giant branch and became a naked helium star. The helium star subsequently evolved to become a CO WD at 299 Myr, losing some mass in the process which explains the decrease in binding energy. The DWD resided in the core of the cluster and experienced a strong perturbation to its orbit shortly after formation which caused the orbit to *harden*. The perturbation did not induce any noticeable eccentricity in to this already circular orbit. Gravitational radiation then removed orbital angular momentum from the system, causing the two WDs to spiral together, until they merged at ~ 630 Myr. Without the perturbation to its orbit the period of this DWD binary would not have been short enough for gravitational radiation to be efficient.

The binary shown in the lower panel of Figure 1 is the DWD formed at 1192 Myr in the second of the $Z = 0.02$ simulations (last entry in Table 1). This binary is the result of a 3-body exchange interaction which occurred at ~ 620 Myr. The binary involved in the exchange is a primordial binary that had experienced two common-envelope events and was

itself a DWD at the time of exchange (see the second entry in Table 2 for Simulation 4). The incoming star had a mass of $2.02M_{\odot}$ and after spending a short time as a quasi-stable 3-body system the least massive star, the $0.82M_{\odot}$ WD in the primordial, was ejected from the system to leave a MS-WD binary with an eccentricity of 0.63 and an orbital period of 14 125 d. This binary was significantly perturbed at 914 Myr (increasing the eccentricity to 0.94) and then experienced a series of common-envelope phases (with the orbital eccentricity having been removed by tidal friction prior to the first CE event) before forming the SNIa candidate of interest at 1 192 Myr. It bears repeating that possible SNIa systems of this sort never occur naturally in the field.

In Table 2 we list all DWDs which are *not* SNIa candidates. This is because the total system masses are less than M_{Ch} , or the merger timescale is longer than a Hubble time, or both. The large numbers of objects demonstrate the rich variety of DWDs created in clusters. It is particularly remarkable that 93 of the 135 binaries listed in Table 2 were created in exchange interactions. This highlights a second key result of our paper: *most of the DWDs in star clusters, and possibly those in the field if they were born in clusters, have progenitors with companions different from the ones we observe today. Furthermore, the orbital period and mass ratio distributions of such objects cannot be reliably predicted without including the effects of dynamics and thus, exchanges.* This is particularly important in comparing the results of observational searches for “loaded guns” with theoretical population predictions (Saffer, Livio & Yungelson 1998). The number of DWDs formed from primordial binaries in the simulations matches well the predicted numbers from the non-dynamical population synthesis. This is also true of the SNIa candidates in Table 1 where the population synthesis predicted either 0 or 1 candidate per simulation.

The histogram of all DWD masses is shown in Figure 2. The distribution of DWDs which will merge in less than a Hubble time is quite similar to that of the DWDs with $M_{\text{b}} > M_{\text{Ch}}$. This is also clear from the histogram of all DWD periods, shown in Figure 3. These confirm that the hardening process does not preferentially act on more massive binaries.

The color-magnitude diagrams of the clusters we have simulated are shown in Figures 4-5 for the $Z = 0.004$ and $Z = 0.02$ models at 1 Gyr intervals. In addition to the single star and binary main-sequences, several blue stragglers and cataclysmic variables (CVs, below and to the left of the MS) are visible in each simulation. The latter have hardly been searched for in open clusters, and this work suggests that systematic searches might be rewarded. Most remarkable are the DWDs, seen in profusion above the white dwarf cooling sequence, and the “loaded guns” shown as circled diamonds in each of the figures.

Figure 6 illustrates the spatial distribution within the cluster at several epochs for the single stars, binaries and DWDs. This clearly demonstrates that the quest for equipartition

of energy is dominating the dynamical evolution: heavy objects segregate towards the inner regions of the cluster while lighter objects move outwards. Binaries are on average more massive than single stars and are therefore more centrally concentrated. Furthermore, the progenitor of any DWD was originally at least twice as massive as the cluster MS turn-off mass at the time the DWD formed, i.e. the DWDs form from the high-end of the binary IMF. This explains why DWDs are more centrally concentrated than the other binaries and means that they are most likely to be found in the core of the cluster, especially those with $M_b > M_{\text{Ch}}$.

4. Accreting Single White Dwarfs

Table 3 lists the possible ASDs generated in our simulations. As with the DWDs, we see that about 2/3 of these binary systems have been involved in exchange interactions. Most are giant-CO-WD pairs, but examples of He and ONe white dwarfs orbiting giants are also present. The number of ASDs is comparable to that predicted by population synthesis without dynamical interactions (~ 6 per simulation) but considering that only 1/3 of the ASDs evolved from primordial binaries it appears that dynamical interactions are destroying as many systems as are being created.

The ASDs are only listed as *possible* because they all have $q > 1$ which, according to most prescriptions for mass transfer, will lead to common-envelope evolution and not steady transfer of material onto the WD (see Section 2). For these systems to become super-soft sources (and possibly SNIa) the common-envelope phase must be avoided, otherwise a DWD, or possibly a single giant, will result. The number of possible ASDs with $q < 1$ at the onset of mass transfer predicted by population synthesis is only ~ 0.4 per simulation which agrees with what we found. However, there is a fair amount of uncertainty in the value of q_{crit} , the mass-ratio above which mass transfer from a giant proceeds on a dynamical timescale. Webbink (1988) presents an expression for q_{crit} which differs by more than a factor of two compared to the model of Hurley, Tout & Pols (2002) for certain values of the giant envelope mass, and which gives $q_{\text{crit}} > 2$ as the envelope mass becomes small. Furthermore, Yungelson & Livio (1998) have shown that the assumption of a strong optically thick wind from the accreting star can act to stabilize the mass transfer. If we allow all values of q_{crit} to lead to stable mass transfer (on a thermal timescale), and assume that all of the transferred material is accreted by the WD, then Table 3 shows that ~ 8 WDs per simulation will reach the M_{Ch} and explode.

5. Discussion

The key result of this paper is that each of the possible progenitors of SNIa is preferentially manufactured in star clusters by orbital hardening and/or exchange interactions. Consequently, in the dense environment of a star cluster, it is binaries altered by, or created from, dynamical interactions that provide the dominant formation channel for short-period DWDs and possible ASDs.

5.1. SNIa Locations

An overly simple prediction based on our results is that we might thus expect to see many or most Type Ia supernovae erupting in star clusters, often in their cores. There are two reasons to be cautious with this prediction.

First, open star clusters disperse, usually on a 1 – 6 Gyr timescale. Stars evaporate from clusters as they acquire energy from other cluster stars, as the Galactic tidal field incessantly tugs at cluster outliers, and through encounters with Giant Molecular Clouds. Second, we don’t know what fraction of stars are created in star clusters, and what fraction of those escape during the earliest stages of cluster life. Observationally checking this prediction is difficult because only a dozen or so SNeIa have been identified closer than the Coma Cluster. Crowding will make at least some SNeIa appear “close” to star clusters, even if they are separated by hundreds of parsecs.

5.2. Globular Clusters

At first glance, performing simulations of globular clusters should act to amplify the effects of dynamical interactions on the stellar populations within the cluster. These simulations will operate at higher particle density and thus the rate of stellar encounters will increase. However, in some cases, this may have the effect of closing production channels. Consider the ASD systems which comprise a Roche-lobe filling giant star and a WD secondary. For such a system to evolve to become a SNIa mass transfer onto the WD must be stable for a significant length of time. Observations of globular clusters (Guhathakurta et al. 1998, for example) show that bright giants are depleted in the core of the cluster indicating that they have been involved in collisions, a consequence of their relatively large cross-section. Such collisions could act to reduce the incidence of stable mass transfer from giants in a globular cluster, either by interrupting the mass transfer or preventing it from occurring at all. On the other hand, short-period DWD systems present a relatively small

cross-section for collision so the increased stellar density should lead to an increased number of weak encounters. The orbital perturbations resulting from these will enhance the likelihood of DWD merger events.

5.3. SNIa Birthrates

The predicted Galactic birthrate of SNeIa from merging supra-Chandrasekhar DWDs is found by Hurley, Tout & Pols (2002) to be $2.6 \times 10^{-3} \text{ yr}^{-1}$. This number is calculated from population synthesis of isolated binaries using the same input parameters to the binary evolution model as used in our NBODY4 simulations. Alternatively, if the Gaussian period distribution for nearby solar-like stars found by Duquennoy & Mayor (1991) is used to determine the initial orbits of the binaries, this number changes by less than 4%. A similar rate is found by Tutukov & Yungelson (1994) using an independent binary evolution algorithm. The observed rate is $4 \pm 1 \times 10^{-3} \text{ yr}^{-1}$ (Cappellaro et al. 1997) so clearly a factor of 10 increase in the predicted rate would bring binary evolution models into conflict with observations. However, Hurley, Tout & Pols (2002) found that if they draw the binary component masses independently from a single star IMF, rather than using a uniform mass-ratio distribution, the predicted rate drops by at least a factor of 10. So the enhancement of SNIa candidates found in our open cluster simulations would allow agreement for the more general mass-ratio distribution when trying to match the results of binary population synthesis studies to observations.

There are additional parameters intrinsic to the binary evolution algorithm which can also affect the production rate of DWDs. The common-envelope efficiency parameter is a prime example. Reducing α_{CE} from 3.0 to 1.0 makes it harder to form short-period binaries via the common-envelope channel and indeed, Hurley, Tout & Pols (2002) found that this also decreased the predicted birthrate of SNeIa from merging supra-Chandrasekhar DWDs by a factor of 10. Because the critical mass-ratio for dynamical mass transfer affects the frequency of common-envelope events, uncertainty in its value (see previous section) will similarly affect any predicted number. Trying to constrain the input parameters to a model of binary evolution by matching the results of binary population synthesis to observations of particular stellar populations is a risky business. The number of uncertain parameters is large and it is entirely possible that an error in one value will mask the error in another. But the key result of this paper remains: hardening of binaries occurs only in clusters, and this preferentially creates SNIa candidates.

5.4. Binary Fraction

Clearly the number of DWD binaries produced in the simulations would increase if we had used a higher binary fraction. The fraction of 10% is a rather conservative choice and we note that in some open clusters it has been found that binaries may be as, or even more, populous than single stars (Fan et al. 1996, for example). We cannot stress enough however (this goes for the discussion in the previous paragraph as well) that it is the number of close DWDs produced in the simulations *relative* to the number produced in the field that is of primary interest in this work. Binaries do present a greater cross-section for dynamical interaction than do single stars (Heggie, Hut & McMillan 1996) so a higher binary fraction does have the capacity to affect the simulation results. This will be addressed in future work.

5.5. Eccentricity

The treatment of gravitational radiation used in the binary evolution algorithm contains a strong dependence on orbital eccentricity, i.e. the removal of angular momentum from the short-period system is accelerated if the orbit is eccentric. Binaries emerging from a common-envelope phase are assumed to be circular so the only way for a short-period DWD orbit to be eccentric is through dynamical interactions subsequent to DWD formation. However, inducing an eccentricity in to an already circular orbit, especially in the case of small orbital separation, is difficult (Heggie & Rasio 1996). In none of the four simulated SNIa candidates that required perturbations to the orbit of a DWD was a detectable eccentricity induced as part of the hardening process.

On a related matter, Hurley et al. (2001) have shown that the shape of the eccentricity distribution used for the primordial binary population can affect the number of blue stragglers produced from that population, for example. This is less important in the case of DWD binaries as the systems of interest will simply form from a slightly different set of primordial binaries. The same goes for variations in the way that tidal friction is modelled (see Hurley, Tout & Pols 2002 for a detailed discussion).

5.6. DWDs and CVs in Clusters

Another intriguing suggestion from this work is that DWDs of all periods should be rather commonplace in open clusters, and likely segregated towards the cluster centres. A significant fraction of these DWDs must have been involved in exchange interactions. We encourage observers to survey for such objects. In the case of CVs we do not find a similar

enhancement in open clusters: typically 1 – 2 CVs were formed in each simulation. We expect that this is mainly due to the required presence of a low-mass MS star, less massive than its WD companion, in any binary that will evolve to a long-lived, and thus stable, CV state. This means that the progenitors of CVs will on average be less massive than the progenitors of DWDs, either on the ZAMS or after the WD (or WDs) have formed, so that they are less likely to reside in the core of the cluster and be involved in dynamical interactions. Furthermore, in a 3-body exchange interaction, it is normally the least massive star that is ejected so CVs are unlikely to form in this manner. We do not rule out the possibility that CV production will be enhanced in simulations of globular clusters. We also note that if merging supra-Chandrasekhar DWDs lead to the formation of neutron stars via an AIC then they are still extremely interesting objects in terms of the neutron star retention problem in star clusters (Pfahl, Rappaport & Podsiadlowski 2002).

6. Conclusions

We find a greatly increased rate of production of “loaded guns” - supra-Chandrasekhar double-white-dwarfs with inspiral ages shorter than a Hubble time - in star clusters relative to the field. Orbital hardening and exchange interactions are the responsible mechanisms for the enhanced rates. Neither of these processes operates in the field, and neither has been included in previous population studies of SNIa progenitors.

The production rate of possible accreting single degenerates is not significantly enhanced relative to the field. However, a major fraction of these systems are formed in exchange interactions, which means that modelling of the stellar dynamics is destroying production channels as well as creating them. Whether or not accreting single degenerates will evolve to become super-soft sources, and ultimately type Ia supernovae, depends critically on avoiding the phase of common-envelope evolution that occurs if mass transfer proceeds on a dynamical timescale.

The results are based on studies of open cluster size N -body simulations, but we expect the effect to be even stronger in the case of globular clusters. The more frequent encounters in globulars will harden DWDs much more rapidly than in open clusters, and hence increase the predicted rate of creation of SNIa progenitors. An increased rate of collisions involving giant stars will deplete the numbers of accreting single degenerate binaries.

We are extremely grateful to Jun Makino and the University of Tokyo for the loan of the GRAPE-6 board. The generous support of Doug Ellis and the Cordelia Corporation has enabled AMNH to purchase new GRAPE-6 boards and we are most grateful for that. MS

thanks Ken Nomoto for very helpful discussions and suggestions. We thank Fred Rasio and Vicky Kalogera for organizing the 2001 Aspen Center for Physics meeting on Star Clusters where some of the ideas for this paper were clarified. We also thank the referee for comments that greatly improved certain aspects of this manuscript.

REFERENCES

- Aarseth, S., Hénon, M., & Wielen, R. 1974, *A&A*, 37, 183
- Aarseth, S. J. 1999, *PASP*, 111, 1333
- Cappellaro, E., Turatto, M., Tsvetkov, D.Yu., Bartunov, O.S., Pollas, C., Evans, R., & Hamuy, M. 1997, *A&A*, 322, 431
- Chen, K., & Leonard, P.J.T. 1993, *ApJ*, 411, L75
- Chernoff, D.F., & Weinberg, M.D. 1990, *ApJ*, 351, 121
- Duquennoy, A., & Mayor, M. 1991, *A&A*, 248, 485
- Eggleton, P.P. 2002, *Evolutionary Processes in Binary and Multiple Stars*, (Cambridge: Cambridge University Press), in preparation
- Eggleton, P.P., Fitchett, M., & Tout C.A. 1989, *ApJ*, 347, 998
- Fan, X., et al. 1996, *AJ*, 112, 628
- Giersz, M., & Heggie, D.C. 1997, *MNRAS*, 286, 709
- Guhathakurta, P., Webster, Z.T., Yanny, B., Schneider, D.P., & Bahcall, J.N. 1998, *AJ*, 116, 1757
- Heggie, D.C. 1975, *MNRAS*, 173, 729
- Heggie, D.C., Hut, P., & McMillan, S.L.W. 1996, *ApJ*, 467, 359
- Heggie, D.C., & Rasio, F.A. 1996, *MNRAS*, 282, 1064
- Hurley, J.R., Pols, O.R., & Tout, C.A. 2000, *MNRAS*, 315, 543
- Hurley, J. R., Tout, C. A., Aarseth, S. J., & Pols, O.R. 2001, *MNRAS*, 323, 630
- Hurley, J.R., Tout, C.A., & Pols, O.R. 2002, *MNRAS*, 329, 897
- Hurley, J.R., & Shara, M.M. 2002, *ApJ*, in press
- Iben, I.-Jr., & Livio, M. 1993, *PASP*, 105, 1373
- Kraft, R. P. 1983, *Highlights in Astronomy*, 6, 129
- Kroupa, P., Tout, C. A., & Gilmore, G. 1991, *MNRAS*, 251, 293

- Kroupa, P., Tout, C. A., & Gilmore, G. 1993, MNRAS, 262, 545
- Kurucz R.L. 1992, in IAU Symposium 149, The Stellar Populations of Galaxies, ed. B. Barbuy, & A. Renzini (Dordrecht: Kluwer), 225
- Lada, E. A., Strom, K. M., & Myers, P. C. 1993, in Protostars and Planets III, ed. E. Levy, & J. Lunine (University of Arizona), 245
- Leibundgut, B. 2001, ARA&A, 39, 67
- Makarov, V.V., & Fabricius, C. 2001, A&A, 368, 866
- Makino, J. 2001, in ASP Conf. Ser. XX, Stellar Collisions, Mergers and their Consequences, ed. M. M. Shara (San Francisco: ASP), in press
- Mardling, R.A., & Aarseth, S.J. 2001, MNRAS, 321, 398
- Perlmutter, S., et al. 1999, ApJ, 517, 565
- Pfahl, E., Rappaport, S., & Podsiadlowski, Ph. 2002, ApJ, submitted
- Phillips, M.M. 1993, ApJ, 413L, 105
- Portegies Zwart, S.F., & Verbunt F. 1996, A&A, 309, 179
- Riess, A.G. et al. 1998, AJ, 116, 1009
- Riess, A.G. 2000, PASP, 112, 1284
- Saffer, R.A., Livio, M., & Yungelson, L.R. 1998, ApJ, 502, 394
- Saio, H., & Nomoto, K. 1998, ApJ, 500, 388
- Tout, C.A., Aarseth, S.J., Pols, O.R., & Eggleton P.P. 1997, MNRAS, 291, 732
- Tout, C.A., Regös, E., Wickramasinghe, D., Hurley, J.R., & Pols, O.R. 2001, in ASP Conf. Ser. 229, Evolution of Binary and Multiple Star Systems: A Meeting in Celebration of Peter Eggleton's 60th Birthday, ed. Ph. Podsiadlowski, S. Rappaport, A. R. King, F. D'Antona, & L. Burder, (San Francisco: ASP), 275
- Tutukov, A., & Yungelson, L. 1994, MNRAS, 268, 871
- Tutukov, A., & Yungelson, L. 1994, MNRAS, 280, 1035
- Webbink R.F. 1998, in IAU Colloquim 103, The Symbiotic Phenomenon, ed. J. Mikolajewska, M. Friedjung, S.J. Kenyon, & R. Viotto (Dordrecht: Kluwer), 311

Yungelson, L., & Livio, M. 1998, ApJ, 497, 168

Yungelson, L., & Livio, M. 2000, ApJ, 528, 108

Yungelson, L., Livio, M., Truran, J.W., Tutukov, A., & Federova, A.V. 1996, ApJ, 466, 890

Table 1. Double-WD systems that are Type Ia candidates. To qualify the system must have a combined mass in excess of the Chandrasekhar mass, $1.44M_{\odot}$, and a gravitational radiation merger timescale less than the age of the Universe, $\sim 1.2 \times 10^{10}$ yr. The time at formation for the double-WD (DWD) system, Myr units, is given in Column 1. The types of the WDs are listed in Column 2. Three types of WD are distinguished: helium composition (He), carbon-oxygen (CO), and oxygen-neon (ONe). The individual masses of the two WDs are given in Columns 3 and 4 respectively, and the combined mass is given in Column 5. All masses are in solar units. The period of the binary is given in Column 6 in units of days. Column 7 gives an estimate of the time it will take the DWD system to merge, in yrs, owing to angular momentum loss from gravitational radiation. This estimate comes from integrating eq. (48) of Hurley, Tout & Pols (2002). Column 8 summarizes the history of each system using the following code: primordial binary (PRIM); exchange interaction (EXCH); perturbation before (PB), or after (PA), Double-WD formed; subsequent escape from cluster (ESC); subsequent disruption in dynamical encounter (DISR). Note that perturbations to the orbit are only recorded if they lead to a change in the evolution path of the binary.

T_{form}	Types		M_1	M_2	M_b	Period	T_{grav}	Legend
225	CO	ONe	0.72	1.24	1.96	3.3884×10^{-1}	4.112×10^9	EXCH
186	CO	CO	0.99	0.66	1.65	1.0715×10^{-1}	2.259×10^8	PRIM-PB-ESC
229	CO	CO	0.97	0.67	1.64	1.1482×10^{-1}	2.991×10^8	PRIM-PA-DISR
334	ONe	CO	1.06	0.57	1.63	1.0715×10^{-1}	2.270×10^8	PRIM-PA
370	CO	CO	1.09	0.54	1.63	2.4547×10^{-1}	2.343×10^9	PRIM-PA
221	CO	CO	0.92	0.64	1.56	4.3652×10^{-2}	2.187×10^7	PRIM-ESC
375	CO	CO	0.83	0.67	1.50	1.1220×10^{-1}	2.997×10^8	PRIM
149	CO	CO	0.83	0.66	1.49	8.7096×10^{-3}	3.350×10^5	PRIM-PB-ESC
223	CO	CO	0.97	0.73	1.70	4.8722×10^{-1}	1.195×10^{10}	PRIM
1299	CO	CO	1.07	0.46	1.53	5.1286×10^{-2}	4.563×10^7	EXCH
123	CO	CO	1.16	0.68	1.84	1.0965×10^{-2}	4.633×10^5	PRIM-ESC
112	ONe	CO	1.10	0.67	1.77	1.6596×10^{-2}	1.544×10^6	PRIM-DISR
225	CO	CO	0.95	0.73	1.68	4.7839×10^{-1}	1.169×10^{10}	PRIM-PA
223	CO	CO	1.09	0.71	1.80	4.6800×10^0	1.007×10^{10}	PRIM-PB
259	ONe	CO	1.12	0.66	1.78	4.0738×10^{-1}	6.958×10^9	PRIM
1192	ONe	CO	1.29	0.30	1.59	3.4449×10^{-1}	1.148×10^{10}	EXCH

Table 2. Double-WD systems that are not Type Ia candidates. Formed either from a primordial binary (PRIM) or via an exchange (EXCH) interaction. See Table 1 for an explanation of what each column entails.

T_{form}	Types		M_1	M_2	M_{b}	Period	T_{grav}	Legend
Simulation 1: $Z = 0.004$								
334	ONe	CO	1.30	0.88	2.18	2.2909×10^4	6.804×10^{23}	PRIM
260	CO	CO	1.08	0.89	1.97	6.3096×10^3	6.575×10^{21}	PRIM
4358	CO	CO	0.62	1.26	1.88	3.6308×10^4	8.779×10^{23}	EXCH
2227	CO	CO	0.89	0.90	1.79	3.4674×10^5	3.417×10^{26}	EXCH
557	CO	CO	0.97	0.79	1.76	2.2910×10^2	1.160×10^{18}	EXCH
2858	CO	CO	0.70	1.01	1.71	3.0903×10^5	2.668×10^{26}	EXCH
3600	CO	CO	0.97	0.72	1.69	1.8621×10^2	7.233×10^{17}	EXCH
1819	ONe	He	1.29	0.37	1.66	5.4954×10^0	8.884×10^{13}	EXCH
2116	CO	CO	1.06	0.59	1.65	1.7378×10^2	6.759×10^{17}	EXCH
1001	CO	CO	0.71	0.87	1.58	8.9125×10^3	2.465×10^{22}	EXCH
596	CO	CO	0.69	0.82	1.51	5.1286×10^0	5.872×10^{13}	EXCH
1596	CO	CO	0.83	0.66	1.49	1.0001×10^6	2.352×10^{28}	EXCH
4232	CO	CO	1.07	0.41	1.48	1.9953×10^1	2.944×10^{15}	EXCH
594	CO	CO	0.79	0.67	1.46	5.7544×10^{-1}	2.157×10^{10}	EXCH
1522	CO	CO	0.71	0.71	1.42	8.3176×10^4	1.102×10^{25}	EXCH
4121	CO	CO	0.67	0.63	1.30	5.6234×10^5	2.079×10^{27}	EXCH
1530	CO	CO	0.59	0.70	1.29	2.1380×10^{-1}	2.209×10^9	EXCH
2933	CO	CO	0.70	0.59	1.29	2.5119×10^2	2.515×10^{18}	PRIM
786	CO	CO	0.67	0.61	1.28	1.7378×10^{-1}	1.098×10^9	EXCH
1009	CO	CO	0.73	0.47	1.20	1.4791×10^{-1}	9.000×10^8	EXCH
2784	CO	CO	0.54	0.61	1.15	5.3703×10^1	4.963×10^{16}	EXCH
2487	CO	CO	0.69	0.43	1.12	1.0715×10^1	7.380×10^{14}	PRIM
631	He	CO	0.34	0.77	1.11	2.5704×10^{-3}	2.507×10^4	EXCH
2494	CO	CO	0.47	0.63	1.10	2.0417×10^1	4.123×10^{15}	EXCH
1930	CO	He	0.68	0.40	1.08	1.6596×10^0	8.215×10^{11}	EXCH
1499	CO	He	0.67	0.33	1.00	1.2023×10^{-1}	8.265×10^8	EXCH
2079	CO	CO	0.35	0.64	0.99	2.0893×10^{-2}	7.279×10^6	PRIM
1690	He	CO	0.36	0.62	0.98	1.9055×10^0	9.372×10^{12}	EXCH
4343	CO	CO	0.77	0.20	0.97	1.2303×10^{-1}	1.223×10^9	PRIM
601	He	CO	0.04	0.92	0.96	1.4791×10^{-2}	1.955×10^7	PRIM
3898	CO	CO	0.40	0.55	0.95	7.4131×10^0	3.597×10^{14}	EXCH
1671	He	CO	0.32	0.62	0.94	8.5114×10^{-1}	1.450×10^{11}	PRIM
3007	CO	CO	0.66	0.27	0.93	1.9055×10^{-1}	4.164×10^9	EXCH
2153	CO	CO	0.55	0.35	0.90	1.9498×10^0	1.108×10^{13}	EXCH
2636	CO	CO	0.60	0.30	0.90	8.1283×10^{-1}	1.597×10^{11}	EXCH

Table 2—Continued

T_{form}	Types		M_1	M_2	M_b	Period	T_{grav}	Legend
780	He	CO	0.33	0.51	0.84	1.5849×10^{-2}	4.211×10^6	PRIM
3267	CO	CO	0.68	0.30	0.98	1.1749×10^0	3.638×10^{11}	EXCH
3341	CO	CO	0.32	0.54	0.86	1.5849×10^0	8.390×10^{11}	EXCH
3564	He	CO	0.20	0.53	0.73	7.5858×10^{-2}	3.774×10^8	EXCH
3601	CO	CO	0.48	0.19	0.67	3.9811×10^{-2}	8.338×10^7	EXCH
Simulation 2: $Z = 0.004$								
111	CO	CO	1.21	1.14	2.35	1.5849×10^4	5.843×10^{22}	PRIM
408	CO	CO	1.08	0.87	1.95	2.5119×10^4	2.769×10^{23}	PRIM
259	CO	CO	1.01	0.74	1.75	1.7783×10^0	3.461×10^{11}	PRIM
3489	CO	CO	0.64	1.08	1.72	3.1623×10^4	6.341×10^{23}	EXCH
668	CO	CO	0.77	0.89	1.67	1.3183×10^4	6.171×10^{22}	PRIM
259	CO	CO	0.93	0.73	1.66	1.5136×10^0	2.366×10^{11}	PRIM
2449	CO	CO	0.86	0.78	1.64	3.9811×10^1	1.189×10^{16}	EXCH
593	CO	CO	0.75	0.88	1.62	6.3096×10^1	4.279×10^{16}	PRIM
2672	CO	CO	0.61	0.93	1.55	3.9811×10^4	1.368×10^{24}	EXCH
890	CO	CO	0.88	0.66	1.54	6.6069×10^1	5.497×10^{16}	PRIM
482	ONe	CO	1.04	0.49	1.53	9.7724×10^{-1}	1.152×10^{11}	PRIM
668	CO	CO	0.86	0.65	1.52	1.2882×10^1	7.099×10^{14}	EXCH
1187	CO	CO	0.69	0.80	1.49	6.1659×10^2	2.105×10^{19}	EXCH
1410	CO	CO	0.78	0.68	1.46	1.8197×10^4	1.819×10^{23}	EXCH
1373	CO	CO	0.57	0.86	1.43	3.0200×10^1	7.814×10^{15}	EXCH
2078	CO	CO	0.78	0.63	1.41	1.5849×10^4	1.394×10^{23}	EXCH
1781	CO	CO	0.75	0.65	1.40	1.9498×10^2	1.107×10^{18}	EXCH
222	CO	CO	0.64	0.70	1.34	6.1659×10^{-2}	7.386×10^7	PRIM
2821	CO	CO	0.71	0.62	1.34	1.5136×10^4	1.289×10^{23}	EXCH
259	CO	CO	0.60	0.72	1.32	1.3804×10^{-1}	6.282×10^8	PRIM
1187	CO	CO	0.74	0.58	1.32	4.0738×10^0	3.938×10^{13}	EXCH
2301	CO	CO	0.64	0.62	1.26	2.6303×10^4	6.209×10^{23}	EXCH
1893	ONe	He	1.01	0.24	1.25	3.0200×10^{-1}	8.483×10^9	PRIM
2412	CO	CO	0.62	0.63	1.25	9.7724×10^4	2.049×10^{25}	EXCH
1336	CO	He	0.88	0.37	1.24	2.6303×10^0	1.626×10^{13}	PRIM
2115	CO	CO	0.68	0.54	1.22	2.4547×10^1	5.731×10^{15}	EXCH
408	CO	CO	0.57	0.63	1.21	9.5499×10^{-2}	2.886×10^8	PRIM
1410	CO	CO	0.53	0.68	1.21	1.4125×10^{-1}	7.178×10^8	EXCH
482	CO	CO	0.61	0.57	1.18	1.9055×10^{-1}	1.640×10^9	PRIM
1707	CO	CO	0.83	0.34	1.18	8.3176×10^{-1}	1.010×10^{11}	PRIM

Table 2—Continued

T_{form}	Types		M_1	M_2	M_b	Period	T_{grav}	Legend
2524	CO	CO	0.48	0.65	1.13	1.0000×10^0	1.798×10^{11}	EXCH
2190	CO	He	0.72	0.32	1.04	1.2882×10^0	4.787×10^{11}	EXCH
853	CO	CO	0.40	0.62	1.03	4.3652×10^{-1}	2.404×10^{10}	PRIM
1967	CO	He	0.71	0.31	1.02	2.7542×10^{-1}	7.620×10^9	EXCH
965	He	CO	0.27	0.73	1.00	1.1220×10^{-1}	7.299×10^8	EXCH
3489	CO	He	0.58	0.41	0.99	8.9125×10^0	5.281×10^{14}	PRIM
1893	He	CO	0.34	0.58	0.92	1.5488×10^0	6.997×10^{11}	EXCH
3971	He	He	0.56	0.34	0.90	3.0903×10^{-3}	5.145×10^4	EXCH
2338	CO	He	0.57	0.31	0.88	8.1283×10^{-1}	1.649×10^{11}	EXCH
1744	CO	He	0.56	0.31	0.87	7.2444×10^{-1}	1.193×10^{11}	EXCH
1818	CO	He	0.64	0.20	0.83	3.0200×10^{-2}	3.238×10^7	EXCH
2709	He	He	0.47	0.33	0.79	1.2023×10^0	5.395×10^{11}	EXCH
4046	He	He	0.38	0.23	0.61	1.3490×10^{-1}	2.522×10^9	PRIM
2895	He	He	0.32	0.20	0.52	3.4674×10^{-2}	7.083×10^7	PRIM
Simulation 3: $Z = 0.02$								
112	CO	CO	1.16	1.12	2.28	1.5488×10^3	1.242×10^{20}	PRIM
186	CO	CO	1.01	0.90	1.91	5.0119×10^1	1.751×10^{16}	PRIM
261	CO	CO	0.86	0.94	1.80	9.7724×10^3	2.419×10^{22}	PRIM
298	CO	CO	0.59	0.63	1.21	1.4454×10^{-1}	8.038×10^8	PRIM
373	CO	CO	0.79	0.81	1.60	1.4454×10^4	8.335×10^{22}	EXCH
560	CO	CO	0.77	0.73	1.50	2.2387×10^4	2.994×10^{23}	PRIM
597	CO	CO	0.62	0.71	1.33	1.3804×10^0	2.724×10^{11}	EXCH
597	CO	CO	0.83	0.73	1.56	1.7783×10^4	1.577×10^{23}	EXCH
634	CO	CO	0.83	0.62	1.45	6.1660×10^0	1.054×10^{14}	PRIM
672	CO	CO	0.72	0.61	1.33	2.6915×10^0	1.338×10^{13}	EXCH
784	CO	CO	0.70	0.69	1.39	1.6218×10^2	6.903×10^{17}	EXCH
896	CO	CO	1.16	0.58	1.74	1.1482×10^1	4.486×10^{14}	EXCH
971	CO	CO	0.75	0.65	1.41	7.4131×10^4	8.103×10^{24}	EXCH
1008	CO	CO	0.57	0.70	1.26	2.8184×10^0	1.631×10^{13}	EXCH
1120	CO	CO	0.55	0.67	1.23	9.1201×10^{-1}	1.095×10^{11}	EXCH
1157	CO	He	0.77	0.32	1.09	1.0000×10^{-2}	1.018×10^6	EXCH
1195	CO	CO	0.81	0.55	1.36	1.4125×10^1	1.098×10^{15}	EXCH
1344	CO	CO	0.83	0.83	1.67	2.0893×10^4	2.090×10^{23}	EXCH
1643	CO	CO	0.63	0.55	1.19	3.7154×10^1	1.697×10^{16}	EXCH
1643	CO	CO	0.62	0.63	1.25	1.7783×10^4	2.214×10^{23}	EXCH
1643	CO	CO	0.65	0.43	1.09	7.4131×10^{-2}	1.561×10^8	EXCH

Table 2—Continued

T_{form}	Types		M_1	M_2	M_b	Period	T_{grav}	Legend
1680	CO	CO	0.65	0.62	1.27	2.1380×10^4	3.548×10^{23}	EXCH
2240	CO	CO	0.89	0.34	1.23	9.5499×10^{-1}	1.652×10^{11}	EXCH
2875	He	CO	0.41	0.77	1.17	1.4125×10^1	1.466×10^{15}	EXCH
2913	He	He	0.28	0.41	0.69	4.4668×10^{-1}	3.984×10^{10}	EXCH
3846	He	CO	0.22	0.77	0.99	3.1623×10^{-1}	1.271×10^{10}	EXCH
4108	CO	He	0.71	0.32	1.03	2.6915×10^0	2.324×10^{13}	PRIM
Simulation 4: $Z = 0.02$								
148	CO	CO	1.14	1.00	2.14	6.6970×10^2	1.501×10^{19}	PRIM
445	ONe	CO	1.29	0.82	2.08	9.1018×10^3	1.671×10^{22}	PRIM
222	CO	CO	1.12	0.89	2.01	1.6921×10^2	4.188×10^{17}	PRIM
222	CO	CO	0.90	1.11	2.01	4.6799×10^1	1.360×10^{16}	EXCH
445	CO	CO	1.10	0.84	1.94	3.6207×10^1	7.584×10^{15}	PRIM
743	CO	CO	0.73	0.79	1.52	1.6410×10^4	1.335×10^{23}	EXCH
780	CO	CO	0.70	0.71	1.41	4.3348×10^2	9.235×10^{18}	EXCH
1449	CO	CO	0.70	0.62	1.32	2.8185×10^4	7.184×10^{23}	PRIM
854	He	CO	0.34	0.88	1.22	9.0059×10^{-2}	3.105×10^8	EXCH
1189	CO	CO	0.62	0.60	1.22	1.0313×10^{-1}	3.087×10^8	EXCH
1151	CO	CO	0.39	0.81	1.20	1.8924×10^{-1}	2.205×10^9	EXCH
706	CO	He	0.89	0.30	1.19	8.9975×10^{-2}	3.105×10^8	PRIM
1932	CO	CO	0.58	0.61	1.19	5.6197×10^4	5.139×10^{24}	EXCH
1709	CO	CO	0.60	0.58	1.18	5.3005×10^0	9.472×10^{13}	EXCH
594	CO	CO	0.56	0.59	1.15	1.0130×10^{-1}	3.087×10^8	EXCH
1263	CO	He	0.77	0.29	1.06	1.0082×10^0	2.086×10^{11}	PRIM
3009	He	CO	0.43	0.58	1.01	1.6502×10^1	2.762×10^{15}	EXCH
1635	He	CO	0.23	0.72	0.95	8.8876×10^{-2}	5.445×10^8	EXCH
1523	CO	He	0.59	0.33	0.92	1.6947×10^0	8.297×10^{12}	EXCH
2229	CO	He	0.60	0.31	0.91	5.1021×10^{-1}	4.095×10^{10}	EXCH
2118	CO	CO	0.29	0.59	0.88	6.0328×10^{-1}	6.660×10^{10}	EXCH
2601	CO	He	0.63	0.23	0.86	1.0000×10^{-1}	8.082×10^8	EXCH
1820	He	He	0.22	0.43	0.65	9.4180×10^{-2}	8.318×10^8	EXCH
1151	He	He	0.31	0.32	0.63	9.0011×10^{-2}	7.395×10^8	PRIM
2935	He	He	0.35	0.25	0.60	9.0417×10^{-1}	1.107×10^9	EXCH

Table 3. Potential super-soft sources. Time at onset of mass transfer is given in Column 1, in Myr units, and the stellar types of the stars at this time are listed in Column 2: Roche-lobe filling star is either on the Hertzsprung gap (HG) or the first giant branch (GB). The mass of the sub-giant or giant, the mass of the WD, and the mass-ratio ($q = M_1/M_2$), are given in Columns 3, 4, and 5, respectively. Column 6 shows the resultant mass of the WD if it were to accept all of the mass available in the donor stars envelope at the onset of mass-transfer. All masses are in solar units. The period of the binary is given in Column 7 in units of days. Column 8 summarizes the history of each system using the following code: primordial binary (PRIM); exchange interaction (EXCH); perturbation to orbit before Roche-lobe overflow (PB); steady mass-transfer (SMT); common-envelope evolution (CE). The outcome of CE is the creation of a DWD system, where the giant has become a HeWD, but in cases where the giant core was non-degenerate a naked helium star (HeMS) is the resulting companion.

T_{RLOF}	Types		M_1	M_2	q	M'_2	Period	Legend
222	GB	CO	3.48	1.09	3.19	4.02	5.1941×10^1	PRIM-CE(HeMS)
1630	GB	CO	1.64	0.62	2.65	1.94	2.1042×10^1	PRIM-PB-EXCH-CE
1639	GB	CO	1.64	0.62	2.65	1.89	4.7514×10^1	EXCH-CE
1893	GB	CO	1.56	0.68	2.29	1.89	3.6108×10^1	EXCH-CE
2969	GB	CO	1.34	0.66	2.03	1.77	4.5509×10^0	EXCH-CE
2598	GB	CO	1.41	0.60	2.35	1.71	1.8143×10^1	EXCH-CE
2450	GB	CO	1.44	0.69	2.09	1.70	1.6049×10^2	PRIM-CE
2116	GB	CO	1.50	0.55	2.73	1.68	4.6434×10^1	EXCH-CE
3229	GB	CO	1.31	0.68	1.93	1.68	2.0417×10^1	EXCH-CE
3303	GB	CO	1.30	0.54	2.41	1.50	3.1223×10^1	EXCH-CE
3860	GB	CO	1.24	0.55	2.25	1.36	1.0945×10^2	EXCH-CE
334	HG	CO	4.07	0.57	7.14	3.99	2.3642×10^1	PRIM-CE(HeMS)
1856	GB	ONe	1.57	1.01	1.55	2.33	6.2060×10^0	PRIM-CE
1299	GB	CO	1.77	0.88	2.01	2.28	5.3945×10^1	PRIM-CE
1781	HG	CO	1.57	0.56	2.80	1.92	1.9978×10^0	EXCH-SMT
2153	GB	CO	1.50	0.72	2.08	1.90	2.6303×10^1	EXCH-CE
1707	GB	CO	1.62	0.56	2.89	1.85	2.1828×10^1	EXCH-CE
1858	GB	CO	1.57	0.58	2.71	1.80	3.8619×10^1	EXCH-CE
2301	GB	CO	1.46	0.57	2.56	1.72	2.0297×10^1	EXCH-CE
2672	GB	He	1.40	0.47	2.98	1.53	3.1203×10^1	EXCH-CE
2858	GB	He	1.35	0.32	4.22	1.47	2.2487×10^0	PRIM-CE
672	GB	CO	2.43	0.77	3.16	2.88	6.1260×10^0	EXCH-CE(HeMS)
4070	GB	CO	1.36	0.71	1.92	1.74	4.6309×10^1	PRIM-CE
2875	GB	He	1.51	0.41	3.66	1.64	1.7278×10^1	EXCH-CE
1226	GB	CO	1.98	0.77	2.57	2.43	3.1687×10^1	PRIM-CE
1597	GB	CO	1.80	0.67	2.69	2.27	2.3700×10^0	EXCH-CE
1486	GB	CO	1.86	0.64	2.91	2.23	9.4690×10^0	EXCH-CE
2192	GB	CO	1.64	0.55	2.98	1.91	1.6321×10^1	EXCH-CE
2564	GB	CO	1.55	0.55	2.82	1.90	2.8284×10^0	EXCH-CE
1783	GB	He	1.74	0.35	4.97	1.87	3.5781×10^0	EXCH-CE
2898	GB	He	1.50	0.36	4.17	1.63	6.1525×10^0	EXCH-CE

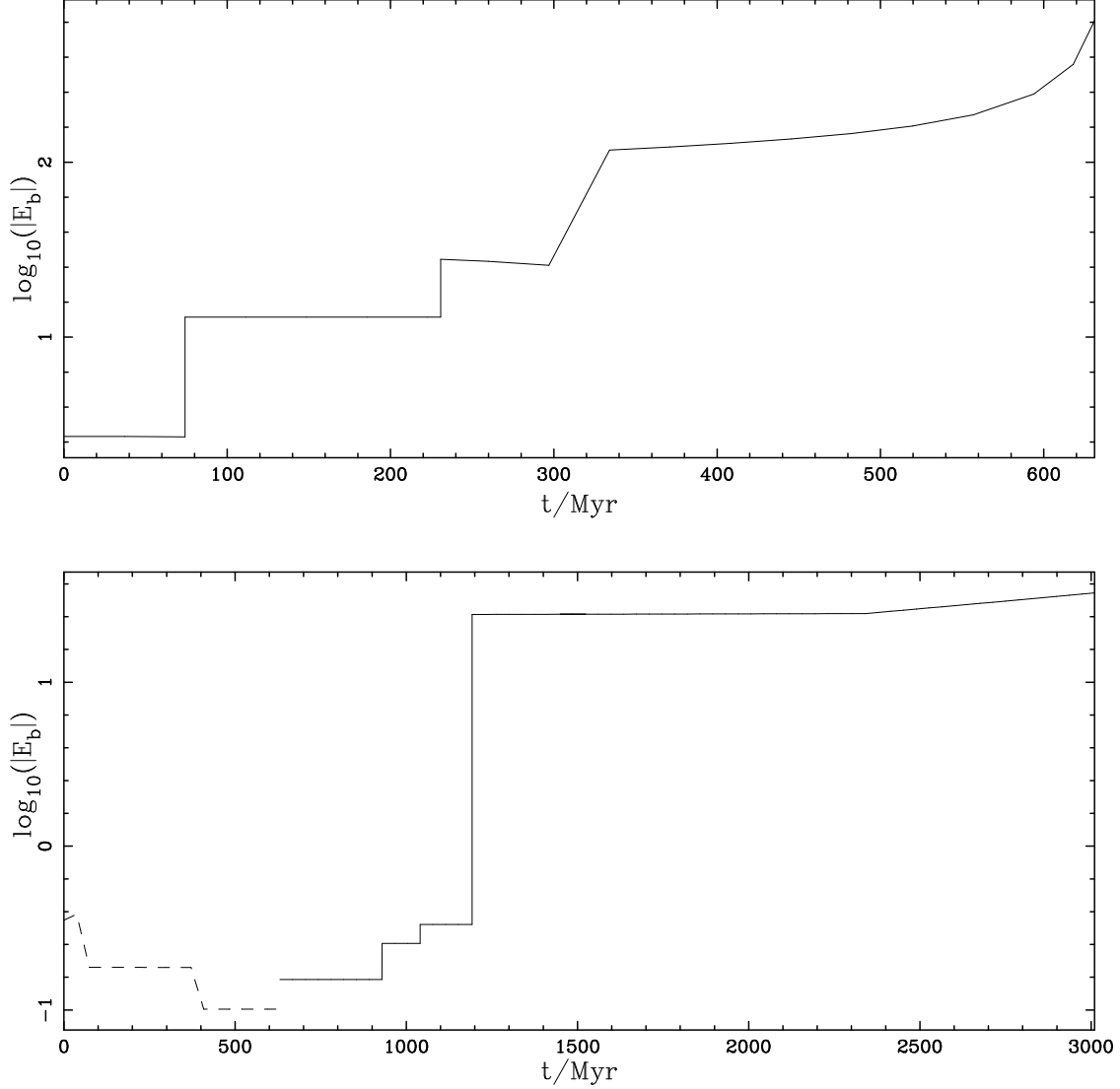


Fig. 1.— The evolution of particular binary systems plotted as the logarithm of the absolute value of the binding energy, E_b , where E_b is in units of M_\odot^2/AU . The top panel shows the ONE-CO DWD formed at 334 Myr in the first $Z = 0.004$ simulation. This system is a possible SNIa candidate (fourth entry in Table 1) and is a primordial binary that had its orbit perturbed after the DWD formed. The system ceases to exist when, at 630 Myr, the two WDs merge to form a supra-Chandrasekhar object. The lower panel shows the ONE-CO DWD formed at 1192 Myr in the second $Z = 0.02$ simulation. This system is also a possible SNIa candidate (last entry in Table 1) and formed in an exchange interaction at 620 Myr. The evolution of the primordial binary involved in the exchange is shown as a dashed line. The evolution after 3000 Myr, in which the two WDs continue to spiral together owing to gravitational radiation, is omitted for clarity.

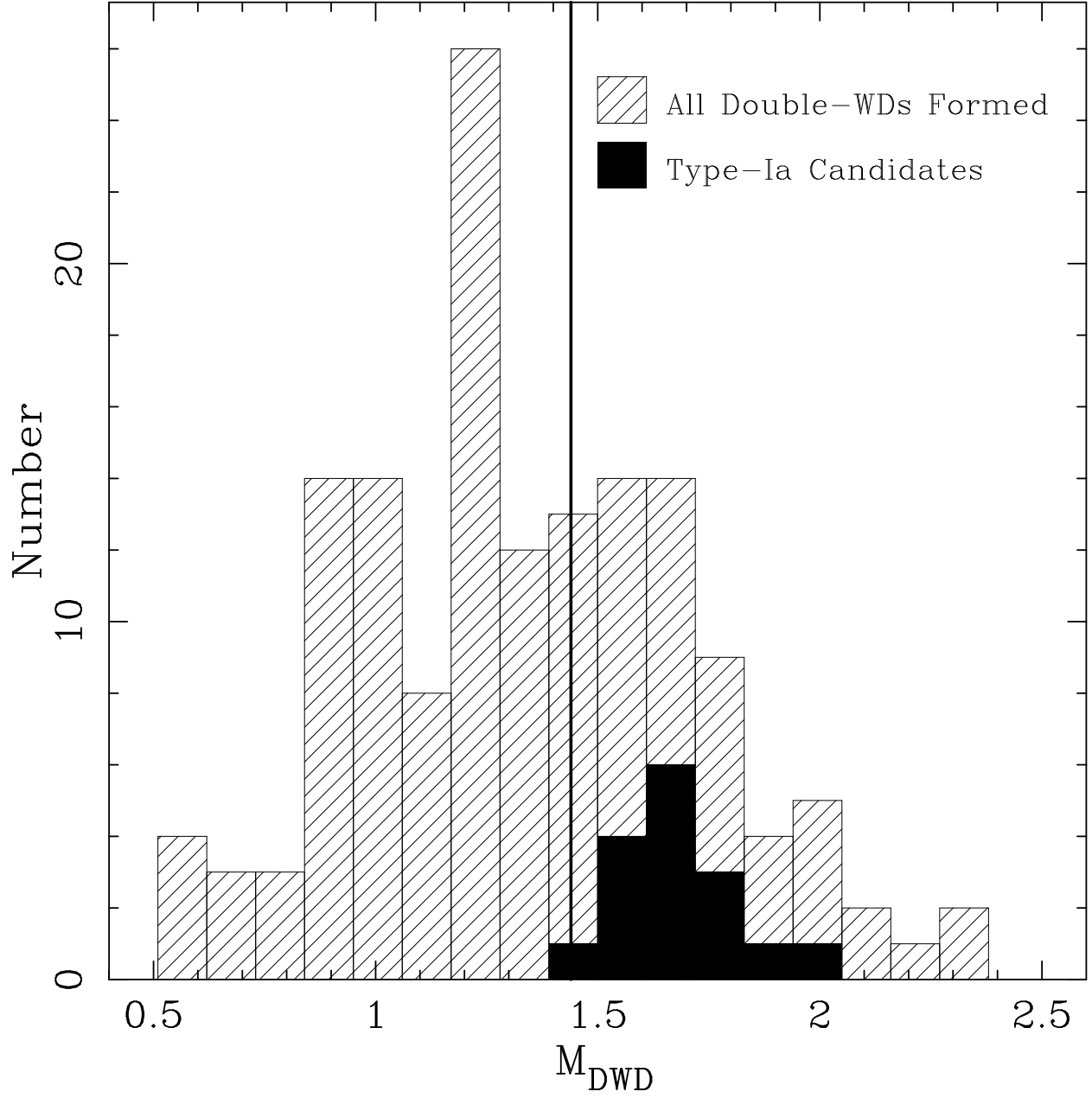


Fig. 2.— Histogram of double-WD masses. The Chandrasekhar mass of $1.44M_{\odot}$ is also shown. All systems listed in Tables 1 and 2 are included.

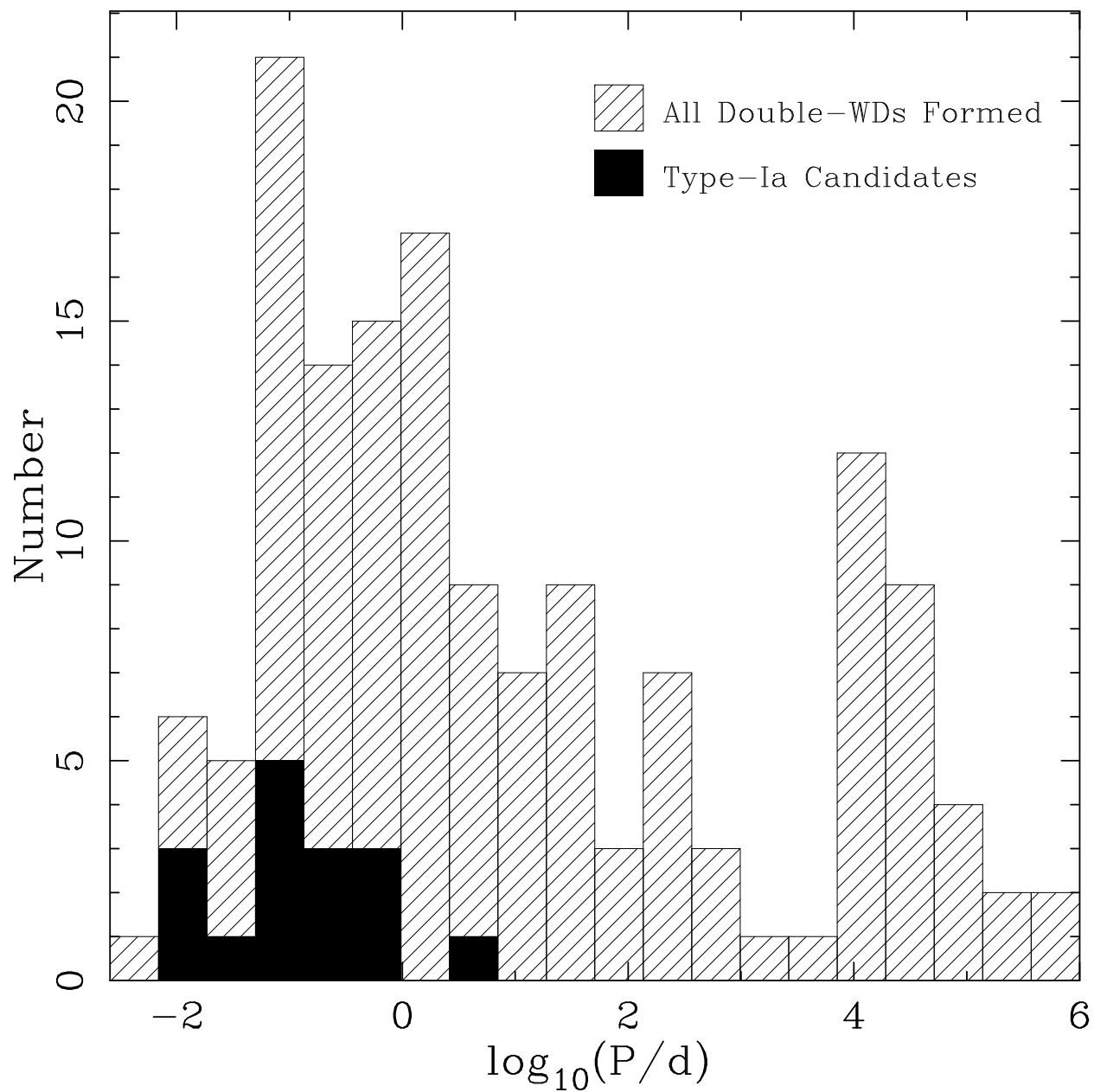


Fig. 3.— Histogram of double-WD periods at the time of formation. All systems listed in Tables 1 and 2 are included.

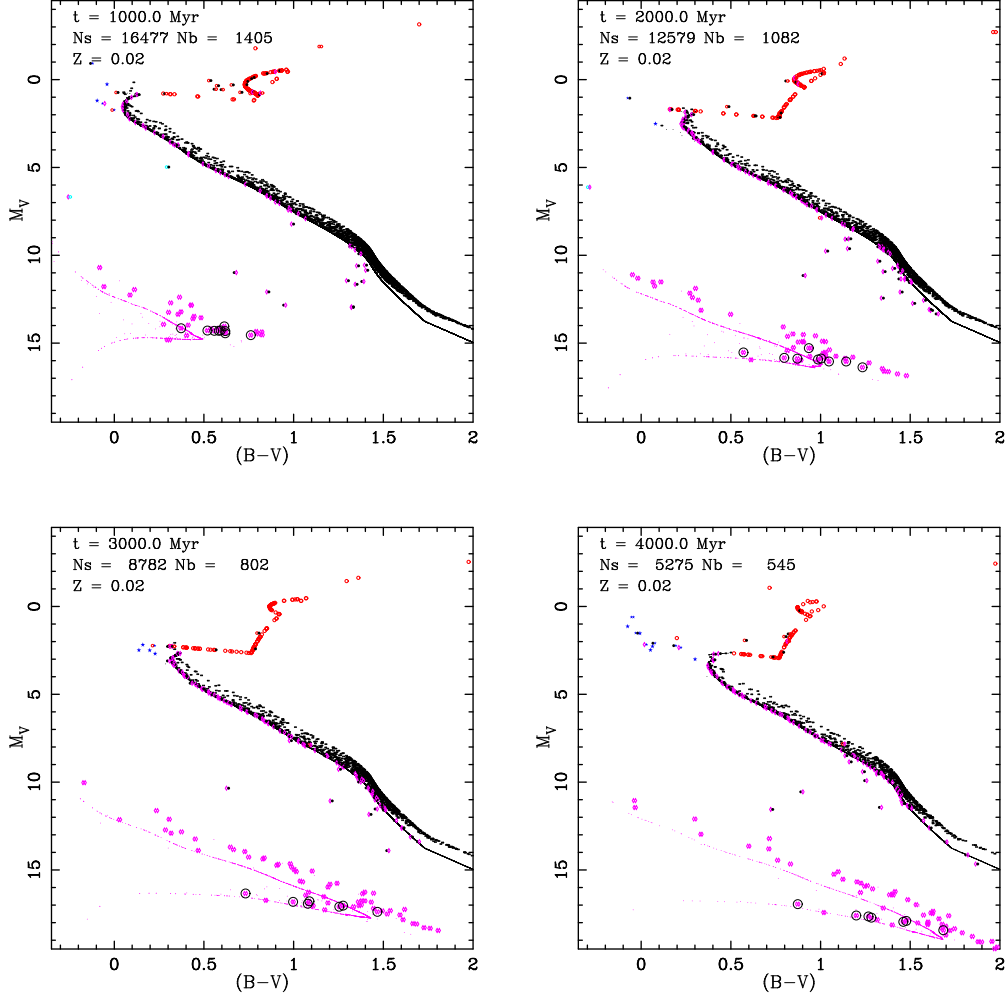


Fig. 4.— Colour-magnitude diagrams for the $Z = 0.004$ simulations at 1.0, 2.0, 3.0 and 4.0 Gyr. Stars from both simulations are plotted but the numbers of single stars and binaries given in each figure are averaged. Main-sequence stars (dots), blue stragglers (stars), sub-giants, giants and naked helium stars (open circles) and white dwarfs (dots) are distinguished. Binary stars are denoted by overlapping symbols appropriate to the stellar type of the components, with main-sequence binary components depicted with filled circles and white dwarf binary components as diamonds. Type Ia candidates are circled. Bolometric corrections computed by Kurucz (1992) from synthetic stellar spectra are used to convert theoretical stellar quantities to observed colours. These corrections are strictly not valid for WDs and extremely cool giants.

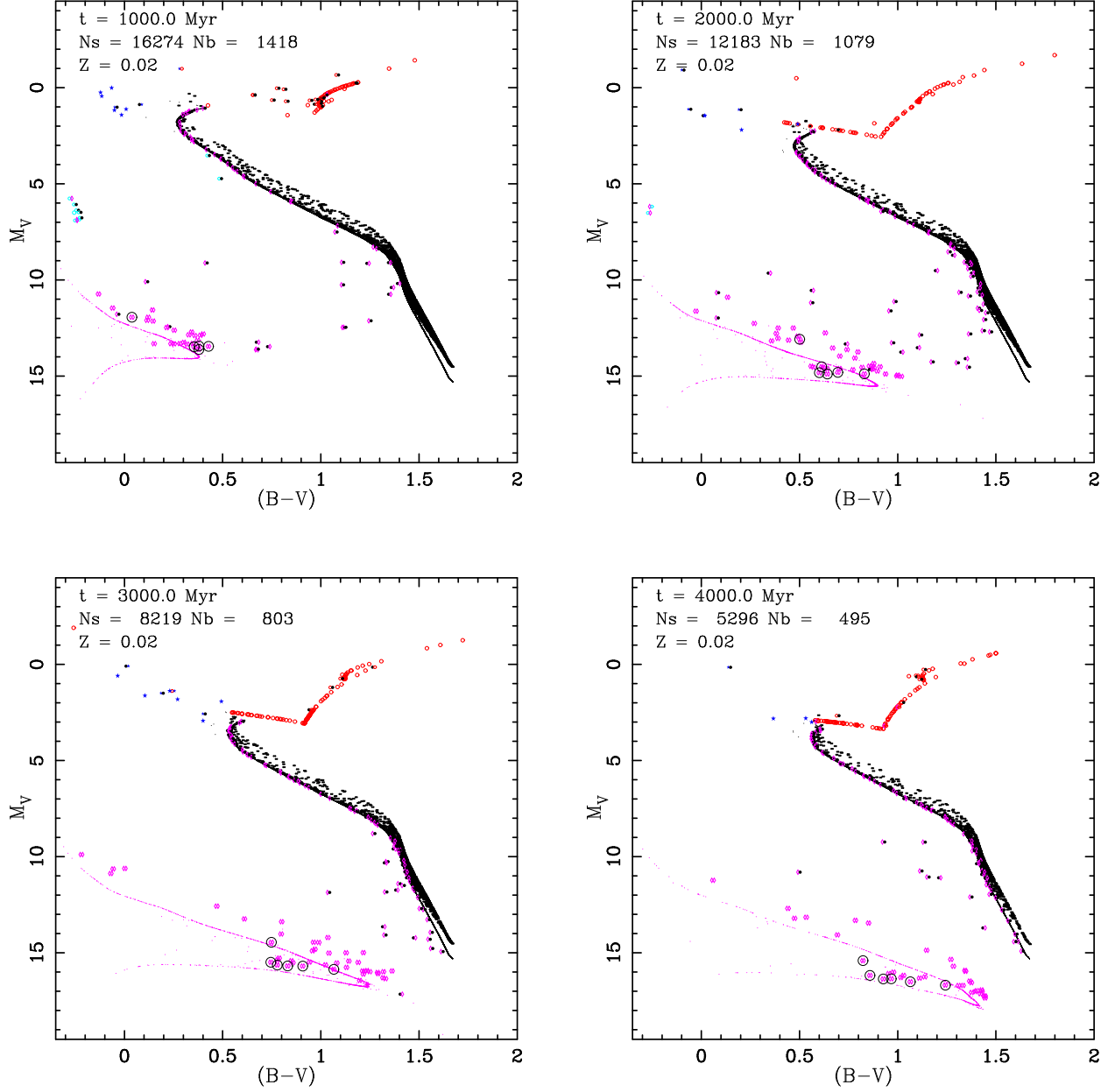


Fig. 5.— Same as Figure 4 but for the $Z = 0.02$ simulations. Note that many of the single main-sequence stars are overlaid by binary stars (in Figure 4 as well).

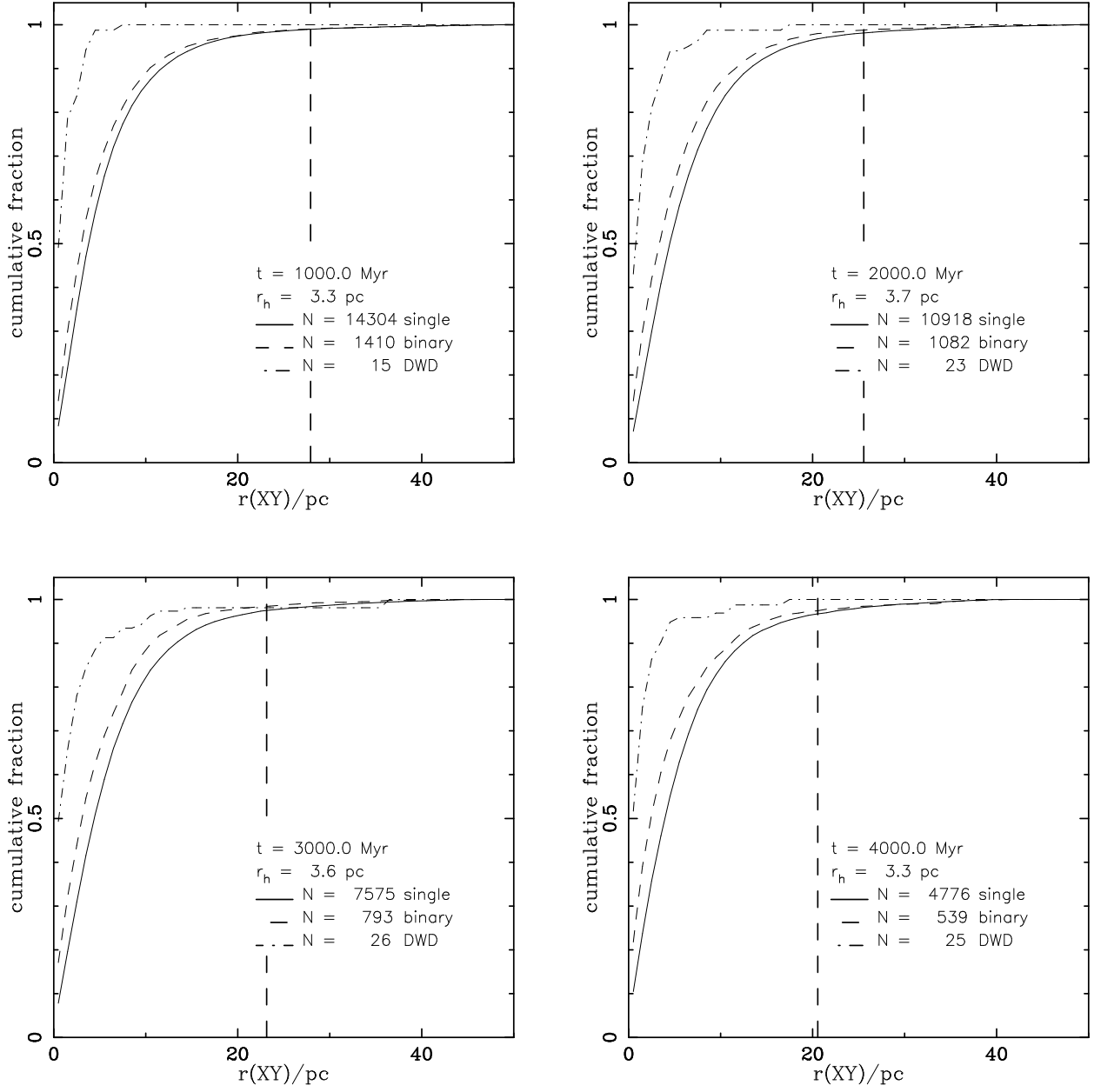


Fig. 6.— Population gradients in the XY-plane for single stars, binaries and double-WDs, averaged over the four simulations presented in this paper. The tidal radius of the cluster is shown as a vertical dashed line. Note that stars are not actually removed from a simulation until they are at a distance greater than two tidal radii from the cluster centre. The half-mass radius, r_h , the tidal radius, and the numbers of each sub-population, are averaged values per simulation.